

RESEARCH

Open Access



# Insertion sequences accelerate genomic convergence of multidrug resistance and hypervirulence in *Klebsiella pneumoniae* via capsular phase variation

Da-Wei Wei<sup>1</sup>, Yuqin Song<sup>1</sup>, Yi Li<sup>1,2</sup>, Gang Zhang<sup>1</sup>, Qi Chen<sup>1</sup>, Linhuan Wu<sup>1</sup>, Jiangqing Huang<sup>1,2</sup>, Xueru Tian<sup>1,3</sup>, Chao Wang<sup>1</sup> and Jie Feng<sup>1\*</sup> 

## Abstract

**Background** The convergence of resistance and hypervirulence in *Klebsiella pneumoniae* represents a significant public health threat, driven by the horizontal transfer of plasmids. Understanding factors affecting plasmid transfer efficiency is essential to elucidate mechanisms behind emergence of these formidable pathogens.

**Methods** Hypermucoviscous *K. pneumoniae* strains were serially passaged in LB medium to investigate capsule-deficient phenotypes. Capsule-deficient mutants were analyzed using genetic sequencing to identify the types and insertion sites of insertion sequences (IS). Bioinformatics and statistical analyses based on the NCBI and National Microbiology Data Center (NMDC) database were used to map the origins and locations of IS elements. Conjugation assays were performed to assess plasmid transfer efficiency between encapsulated and capsule-deficient strains. A murine intestinal colonization model was employed to evaluate virulence levels and IS excision-mediated capsule restoration.

**Results** Our research revealed that a hypervirulent *K. pneumoniae* (hvKP) strain acquired a *bla*<sub>NDM-1</sub>-bearing IncX3 plasmid with IS5 and ISKox3 elements. These IS elements are capable of inserting into capsular polysaccharide synthesis genes, causing a notably high frequency of capsule loss in vitro. The IS-mediated capsular phase variation, whether occurring in the donor or recipient strain, significantly increased the conjugation frequency of both the resistance plasmid and the virulence plasmid. Additionally, capsular phase variation enhanced bacterial adaptability in vitro. Experiments in mouse models demonstrated that capsule-deficient mutants exhibited reduced virulence and colonization capacity. However, during long-term intestinal colonization, IS element excision restored capsule expression, leading to the recovery of hypervirulence and enhanced colonization efficiency.

**Conclusions** Our findings reveal that IS elements mediate capsular phase variation by toggling gene activity, accelerating the genomic convergence of multidrug resistance and hypervirulence in *K. pneumoniae*, as well as facilitating adaptive transitions in different environments.

**Keywords** Carbapenem-resistant hypervirulent *Klebsiella pneumoniae*, Insertion sequence, Capsular phase variation, Genomic convergence

\*Correspondence:

Jie Feng

fengj@im.ac.cn

Full list of author information is available at the end of the article



© The Author(s) 2025. **Open Access** This article is licensed under a Creative Commons Attribution-NonCommercial-NoDerivatives 4.0 International License, which permits any non-commercial use, sharing, distribution and reproduction in any medium or format, as long as you give appropriate credit to the original author(s) and the source, provide a link to the Creative Commons licence, and indicate if you modified the licensed material. You do not have permission under this licence to share adapted material derived from this article or parts of it. The images or other third party material in this article are included in the article's Creative Commons licence, unless indicated otherwise in a credit line to the material. If material is not included in the article's Creative Commons licence and your intended use is not permitted by statutory regulation or exceeds the permitted use, you will need to obtain permission directly from the copyright holder. To view a copy of this licence, visit <http://creativecommons.org/licenses/by-nc-nd/4.0/>.

## Background

*Klebsiella pneumoniae* is a major clinical pathogen known for causing severe organ infections. Its ability to acquire new genetic material facilitates the development of multidrug resistance (MDR) and hypervirulence, each posing unique challenges for clinicians [1]. Multidrug-resistant strains, particularly carbapenem-resistant *K. pneumoniae* (CRKP), represent a critical public health threat [2]. This concern is underscored by their inclusion on the World Health Organization's (WHO) list of priority antimicrobial-resistant pathogens needing new control strategies [3]. Hypervirulent *K. pneumoniae* (hvKP) is notable for causing infections in healthy individuals of all ages, often presenting as hepatic abscesses without biliary tract disease [4]. Initially, hvKP isolates were sensitive to antimicrobials. However, nearly 40 years after its first description, antibiotic-resistant hvKP strains, particularly carbapenem-resistant hypervirulent *K. pneumoniae* (CR-hvKP), have emerged, posing significant clinical challenges [5, 6]. A 2016 study in China revealed that 20 out of 35 (57%) hvKP bloodstream infection isolates produced carbapenemase, highlighting the severity of the issue [7]. Two types of convergence patterns have been identified: CRKP strains acquiring virulence plasmids and hvKP strains obtaining plasmids carrying carbapenem-resistant genes [5, 6, 8, 9]. This convergence of virulence and antibiotic resistance is primarily driven by horizontal gene transfer mediated by plasmids [10]. Understanding the factors influencing plasmid transfer efficiency is crucial to developing strategies for mitigating the spread of these formidable pathogens.

The capsule of *K. pneumoniae* is the initial cellular structure that interacts with the environment. It is primarily studied for its critical role as a virulence factor, as it conceals surface antigens and mitigates the immune response [11]. Recent studies have demonstrated that inactivating genes responsible for capsule synthesis results in a high conjugation frequency of plasmids [10, 12]. Insertion sequence (IS) elements were found to integrate into the capsule gene *wcaJ* in clinical isolates of hvKP, leading to a significant reduction in capsular polysaccharides and an increased conjugation frequency of the *bla*<sub>KPC-2</sub> plasmid [12]. As small transposons encoding transposase enzymes that catalyze the “hopping” event, IS elements induce alterations in the host genome throughout bacterial evolution [13]. While it is well known that IS elements play a crucial role in the dissemination of antibiotic resistance, their impact on the capsular polysaccharide (CPS) synthesis and plasmid transfer efficiency remains largely unexplored. Gaining a deeper understanding of this role is essential for addressing the evolution and spread of these formidable pathogens.

Our findings demonstrate the significant role of insertion sequence (IS) elements in shaping the genome and environmental adaptation of a carbapenem-resistant plasmid acquired by the hypervirulent *K. pneumoniae* strain NK01067. The IS elements on the plasmid can insert into CPS synthesis genes, leading to a markedly high frequency of capsule loss in vitro. The CPS-deficient strain exhibits advantages in growth and biofilm formation. Furthermore, IS-mediated capsule inactivation significantly increases the conjugation frequency of the plasmid—by up to 7.61 log<sub>2</sub>-fold higher in capsule-deficient strains. This consequently facilitates the rapid spread of resistance and virulence plasmids, resulting in the genomic convergence of resistance and virulence traits. Surprisingly, in a mouse model, capsule-deficient mutants can restore CPS through the loss of IS elements in capsule loci, thereby regaining hypervirulence and achieving better colonization in the gut. Our study underscores the dynamic interplay between capsule loss and restoration mediated by IS elements both in vivo and in vitro. It highlights the critical role of IS elements in accelerating the genomic convergence of multidrug resistance and hypervirulence in *K. pneumoniae* by switching genes on and off.

## Methods

### Bacterial strains, culture, and antibiotics

The main bacterial strains and plasmids used for experimental and genetic manipulations in this study are listed in Additional file 1: Table S1. Additionally, Additional file 1: Table S2 provides detailed information on the hypermucoviscous *K. pneumoniae* clinical isolates, including sequence type (ST), capsule locus (KL) type, O-antigen serotypes, antimicrobial resistance genes, virulence factors, insertion sequence elements, isolation sources, and relevant references. All *K. pneumoniae* and *Escherichia coli* strains were cultured in Luria–Bertani (LB) broth or on LB agar plates at 37 °C with shaking at 220 rpm. Antibiotics were supplemented at the following final concentrations: meropenem, 1 mg/L; chloramphenicol, 20 mg/L; kanamycin, 50 mg/L; rifampicin, 100 mg/L; trimethoprim, 50 mg/L; and hygromycin, 100 mg/L.

### Serial in vitro passages and insertion analysis

Each of the three single colonies of hvKP with KL1 or KL2 capsule types was grown overnight in 2 ml of LB medium (marked as 0 h). The cultures were then diluted 1/200 in fresh media every 24 h and incubated at 37 °C. Cultures at 0, 24, 48, and 72 h were serially diluted and colony forming units (c.f.u.) were counted. The ratio of observed non-mucoid translucent (NM-T) colonies to the total number of colonies on the plates was calculated. For strain NK01067 or NK10012, 23 NM-T colonies were

selected and streaked on LB agar. PCR verification was performed using primers for *wcaJ*, *wza*, *wzb*, and *wzc* (Additional file 1: Table S3). IS insertion mutations were determined based on the changed band sizes observed on agarose gel electrophoresis and the subsequent Sanger sequencing.

#### In situ *wcaJ* gene complementation

To establish the *wcaJ*::IS5 complementation strains in situ, a suicide plasmid pDM4-*wcaJ* was constructed as previously described [14]. *WcaJ* was amplified from the wild-type strain NK01067 using the primer pairs listed in Additional file 1: Table S3 and cloned into the pDM4 vector by Gibson assembly, resulting in the plasmid pDM4-*wcaJ*. This plasmid was then transferred into strain *wcaJ*::IS5 via *E. coli* S17-1 ( $\lambda$  *pir*)-mediated conjugation to facilitate a single crossover event. Transconjugants were plated on LB agar supplemented with 20 mg/L chloramphenicol and 2 mg/L meropenem. Counter selection for markerless in-frame deletion was performed on LB agar plates with 15% sucrose.

#### Plasmid extraction and electroporation of pNK01067-NDM-1

Strain NK01067 was grown overnight at 37 °C with shaking at 200 rpm. Five milliliters of cultures was sedimented at 12,000 rpm for 1 min to extract the pNK01067-NDM-1 plasmid using the HiPure BAC Mini Kit (Magen Biotechnology, Guangzhou). *K. pneumoniae* electrocompetent cells were prepared with slight modifications to the previously described method [15]. An overnight culture was diluted 1/100 in fresh LB broth and shaken at 37 °C until  $OD_{600\text{ nm}} = 0.5$ . After 20 min on ice, cells were harvested at 10,000 rpm for 10 min at 4 °C, washed three times with ice-cold sterile double-distilled water, and resuspended in 10% glycerol. Five microliters of pNK01067-NDM-1 plasmid was added to 50  $\mu$ l of electrocompetent cells, and electroporation was performed using the following parameters: 2500 V, 200  $\Omega$ , 25  $\mu$ F. The electroporated cells were recovered in 1 ml of fresh LB broth for 1 h and plated on LB agar containing 4  $\mu$ g/ml meropenem, and incubated at 37 °C overnight.

#### Whole-genome sequencing and bioinformatics analysis

Whole-genome sequencing (WGS) was conducted on DNA extracts from relevant cultures using Illumina NovaSeq 6000 platform. The platform generated high-quality 2 $\times$  150-bp paired-end reads for each sample. SPAdes v3.13.0 was employed for de novo assembly from Illumina data to obtain draft genomes [16]. Mutations in capsule cluster genes were analyzed through sequence alignment. The annotations IS and plasmids were performed using the ISfinder database ([\[ul.fr/about.php\]\(https://isfinder.bioto.fr/about.php\)\) and the plasmidfinder database \(<https://cge.food.dtu.dk/services/PlasmidFinder/>\), respectively \[17, 18\]. Plasmid circular maps were created using the online software Proksee \(<https://proksee.ca/>\) \[19\]. Schematic maps for linear comparisons were generated using EasyFig \(v2.2.2\) \[20\]. Images were adjusted or modified by using Inkscape \(v0.92\) \[21\]. For the analysis of IS5 origin, we firstly downloaded 1791 \*K. pneumoniae\* complete genomes from the NCBI database. BLASTn was conducted to screen the genomes containing IS5, and the information for the location of IS5 \(on chromosome or plasmid\) was further extracted based on the annotation files for each genome \[22\]. Then, multi-locus sequence typing \(MLST\) analysis was performed for the IS5-carrying genomes to determine their STs \[23\]. The co-existence of \*bla\*<sub>NDM</sub>, \*ISKox3\*, and IS5 was detected by the annotations of corresponding genes. For the tracing of IS5 and \*ISKox3\* source and flow, we further collected 285,417 bacterial genomes of 471 pathogenic species from the gcPathogen database. We then performed IS5 and \*ISKox3\* annotations for each genome. The gcPathogen database is a comprehensive genomic resource for human pathogens, curated within the NMDC platform \(<https://nmdc.cn/gcpathogen/pathogens?otherType=taxa&type=bacteria>\) \[24\].](https://isfinder.bioto</a></p></div><div data-bbox=)

#### Plasmid conjugation assay

For all conjugation experiments, the procedure was as described with slight modifications [10]. First, both donor and recipient strains were cultured overnight in LB broth supplemented with the appropriate antibiotics. A 1/100 dilution was then transferred to fresh antibiotic-containing medium and grown to an approximate  $OD_{600\text{ nm}}$  of 0.6. The cultures were centrifuged, washed twice with 10 mM MgSO<sub>4</sub> to remove residual antibiotics, and the cells were adjusted to an  $OD_{600\text{ nm}}$  of 0.2. One milliliter of each cell suspension was mixed, centrifuged, and the supernatant discarded. The pellet was resuspended in 20  $\mu$ l of 10 mM MgSO<sub>4</sub> and inoculated onto LB agar plates. After 24 h of incubation at 37 °C, the bacteria were resuspended and serially diluted in PBS, followed by plating on antibiotic-containing LB agar plates for transconjugant selection. Transconjugants were then confirmed by PCR and sequence analysis. Conjugation frequency was calculated as the ratio of transconjugants to recipients based on c.f.u. counts on serial dilution plates containing the appropriate antibiotics. Each experiment was performed in six independent replicates.

#### Mucoviscosity assay and uronic acid quantitation

Mucoviscosity was determined by a modified sedimentation assay [9]. Overnight LB broth cultures were normalized to  $OD_{600\text{ nm}} = 1.0$  and 1 ml was sedimented at 1000

×g for 5 min. Two hundred microliters of the supernatant was transferred to 96-well plates for OD<sub>600 nm</sub> measurement. Wells containing 200 µl LB broth were used as negative controls. Uronic acid extraction and quantification followed modified protocols [2]. Overnight LB broth cultures (OD<sub>600 nm</sub> = 1.0) were mixed with 100 µl of 1% Zwittergent-100 in 100 mM citric acid and incubated at 50 °C for 20 min. After centrifuging at 13,000 rpm for 5 min, 300 µl of the supernatant was mixed with 1.2 ml of ethanol, incubated at 4 °C for 20 min, and centrifuged again. The pellet was resuspended in 200 µl of water, mixed with 1.2 ml of 12.5 mM sodium tetraborate in sulfuric acid, incubated at 100 °C for 5 min, and cooled on ice. Absorbance at 520 nm was measured after adding 20 µl of 0.15% 3-phenylphenol in 0.5% NaOH. Glucuronic acid content was determined using a standard curve and expressed as micrograms per OD unit.

### Biofilm analysis

The biofilm formation assay followed modified protocols [2]. Overnight LB broth cultures were grown at 37 °C with shaking at 200 rpm, then diluted 1:1000 in LB broth. One hundred fifty microliters of each culture was inoculated into 6 wells of a 96-well plate and incubated stationarily at 30 °C for 24 h. After incubation, 100 µl was removed for OD<sub>600 nm</sub> measurement to assess cell growth. Each well was then stained with 200 µl of 1% crystal violet for 30 min, rinsed five times with deionized water, and solubilized with 250 µl of 80% ethanol. Two hundred microliters of the solution was transferred to a new plate for OD<sub>590 nm</sub> measurement.

### Growth curves

Overnight cultures were diluted 1:1000, and 200 µl of each diluted culture was transferred to a 96-well microplate. The OD<sub>600 nm</sub> of the cell cultures was measured every 20 min for 24 h using a BioTek Synergy H4 Hybrid multimode microplate reader. Absorbance values from four technical replicates were averaged and used as data points for statistical analysis. Growth rate results were analyzed using paired, two-tailed Student's *t*-tests in GraphPad Prism version 8.

### Animal experiments

All animal experiments were approved by the Ethics Committee of the Institute of Microbiology, Chinese Academy of Sciences (Approval No. APIM-CAS2023077). Six-week-old male specific pathogen-free (SPF) BALB/c mice were procured from Charles River Laboratories Co., Ltd. in Beijing, China. Following a 1-week acclimatization period in a Biosafety Level 2 facility, all experiments were initiated. Mice were housed in individually ventilated cages (IVCs)

with a maximum of five animals per cage under standardized conditions: a 12-h light/dark cycle, ambient temperature maintained at 22–25 °C, and relative humidity of 45–55%. Animals had ad libitum access to autoclaved rodent chow and purified water. All cages were equipped with sterilized bedding, and animal husbandry was performed by trained personnel in accordance with established protocols to ensure animal welfare. Mice were monitored daily for general health and signs of distress. Animals exhibiting weight loss greater than 20% of baseline were humanely euthanized by carbon dioxide inhalation.

### Long-term intestinal colonization model

The overnight cultures of NM-T strain *wcaJ*::IS5 were inoculated to fresh medium and cultivated to an OD<sub>600 nm</sub> of 0.8. After centrifugation at 5000 rpm for 3 min, the cultures were washed twice with PBS and resuspended in PBS to an OD<sub>600 nm</sub> of 1.0. A volume of 100 µl of the suspension was administered to mice by oral gavage at a dose of  $1 \times 10^8$  c.f.u.. Mouse body weights were recorded on days 2, 6, 13, and 28, and fecal samples were collected. For fecal sampling, 2–3 pellets from each mouse were pooled and weighed, thoroughly resuspended in PBS, serially diluted, and plated on Simmons' citrate agar with 1% inositol (SCAI). After incubation at 37 °C for 24 h, *K. pneumoniae* colonies were counted and standardized to determine c.f.u. per gram of feces, with a detection limit of 5000 c.f.u./g. While only one technical replicate was performed for each sample, strict measures were taken to ensure data accuracy. After performing all dilution and plating steps, any evident dilution inconsistencies were addressed by re-diluting the samples to ensure proper dilution and reliable counting. For samples below the detection limit, triplicate counts were performed to confirm reliability. The phenotype of the colonies was also recorded.

### Virulence evaluation in gut infection models

The culture of approximate  $5 \times 10^7$  c.f.u. was used for intestinal infection in the survival experiments. Overnight bacterial cultures were subcultured in LB and grown with shaking at 37 °C to an OD<sub>600 nm</sub> of ~0.8. The cultures were then washed with PBS and resuspended in PBS to an OD<sub>600 nm</sub> of 0.5. A volume of 100 µl of the NK01067, *wcaJ*::IS5, *wcaJ*::IS5/*wcaJ*, and revertant strains was administered orally by gavage. Mouse body weights and mortality rates were recorded. Any animal that lost more than 20% of its original body weight was euthanized by CO<sub>2</sub> inhalation to prevent further suffering.

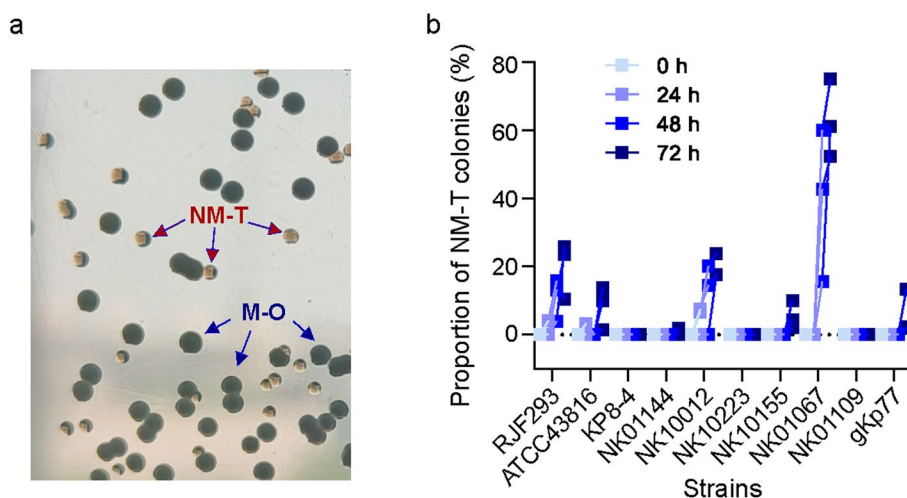


**Fig. 1** CR-hvKP strain NK01067 exhibits a markedly increased frequency of capsular phase variation in vitro. **a** Mucoid opaque (M–O) and non-mucoid translucent (NM–T) colony phenotypes on LB agar. **b** The proportion of NM–T colonies of various clinical hvKP strains after serial passages on LB agar, measured at 0, 24, 48, and 72 h. The experiment was conducted in triplicate independently

## Results

### A CR-hvKP strain exhibits a markedly increased frequency of capsular phase variation in vitro

HvKP typically develop overproduction of the capsule, resulting in colonies with a hypermucoid appearance characterized by a raised center, clean margins, and a smooth, wet surface [25]. In this study, we identified ten hvKP strains originating from diverse clinical sources based on their capsule serotypes (KL1/KL2), the presence of *rmpA* (a regulatory gene that enhances capsule production), and a hyperviscosity phenotype (Additional file 1: Table S2). When plated on LB agar, some strains exhibited two distinct colony types: mucoid opaque (M–O) and non-mucoid translucent (NM–T) (Fig. 1a). To investigate the phase variation pattern, we conducted serial in vitro passages of these ten hvKP strains initially identified as M–O and tracked the proportion of emerging NM–T colonies at 24, 48, and 72 h. The results showed an increasing trend in the proportion of NM–T colonies with successive passages except for strains KP8–4, NK10223, and NK01109 which maintained the M–O phenotype through consecutive subcultures (Fig. 1b). This phenomenon may be attributed to passage in LB medium reducing selection pressure, thereby leading to the loss of high-cost traits such as capsule production [2, 11, 26]. The frequencies of such switch vary greatly among seven strains with phenotypic heterogeneity. NK01067 (ST23, KL1, O1), isolated from a patient's sputum, displayed a significantly high rate of phenotypic switching, with the NM–T colonies reaching an average proportion of 63% at 72 h (Fig. 1b). This strain exhibited high-level carbapenem resistance (meropenem MIC: 64

mg/ml). Subsequent whole-genome analysis identified an IncX3-type resistance plasmid, a major vector for the carbapenem resistance gene *bla*<sub>NDM-1</sub> in the isolate [27]. The *bla*<sub>NDM-1</sub> gene was located on a Tn3000 composite transposon derivative with an IS5 insertion upstream of *bla*<sub>NDM-1</sub> (Additional file 2: Fig. S1). This genetic configuration has been frequently reported in *Escherichia coli* strains from East Asia [28, 29].

### IS element-mediated inactivation of capsular polysaccharide synthesis genes results in high frequency capsule loss

The transition between M–O and NM–T colonies is associated with mutations in the capsular polysaccharide synthesis genes within the CPS loci [2, 11, 30]. Among these, mutations in the *wcaJ* gene, which encodes a glycosyltransferase, were the most common cause of CPS loss [11, 31, 32]. Additionally, the *wzc* gene, encoding tyrosine autokinase, and the *wza* and *wzb* genes, encoding polysaccharide export protein and protein tyrosine phosphatase, are also hotspots for capsule inactivation mutations [31, 32]. To understand the mechanism underlying the high rate of CPS loss in strain NK01067, we amplified fragments of *wcaJ*, *wza*, *wzb*, and *wzc* from 23 NM–T colonies of NK01067 after 72 h of culture. Agarose gel electrophoresis revealed that 87.0% (20/23) of the colonies displayed increased band sizes at the *wcaJ*, *wza*, and *wzc* loci, indicative of IS insertions leading to gene inactivation (Fig. 2a). Sequencing results showed that IS5 had inserted into *wcaJ* in 17 colonies, into *wza* in 1 colony, and ISKox3 had inserted into *wzc* in 2 colonies (Fig. 2a–d and Additional file 1: Table S4). We analyzed

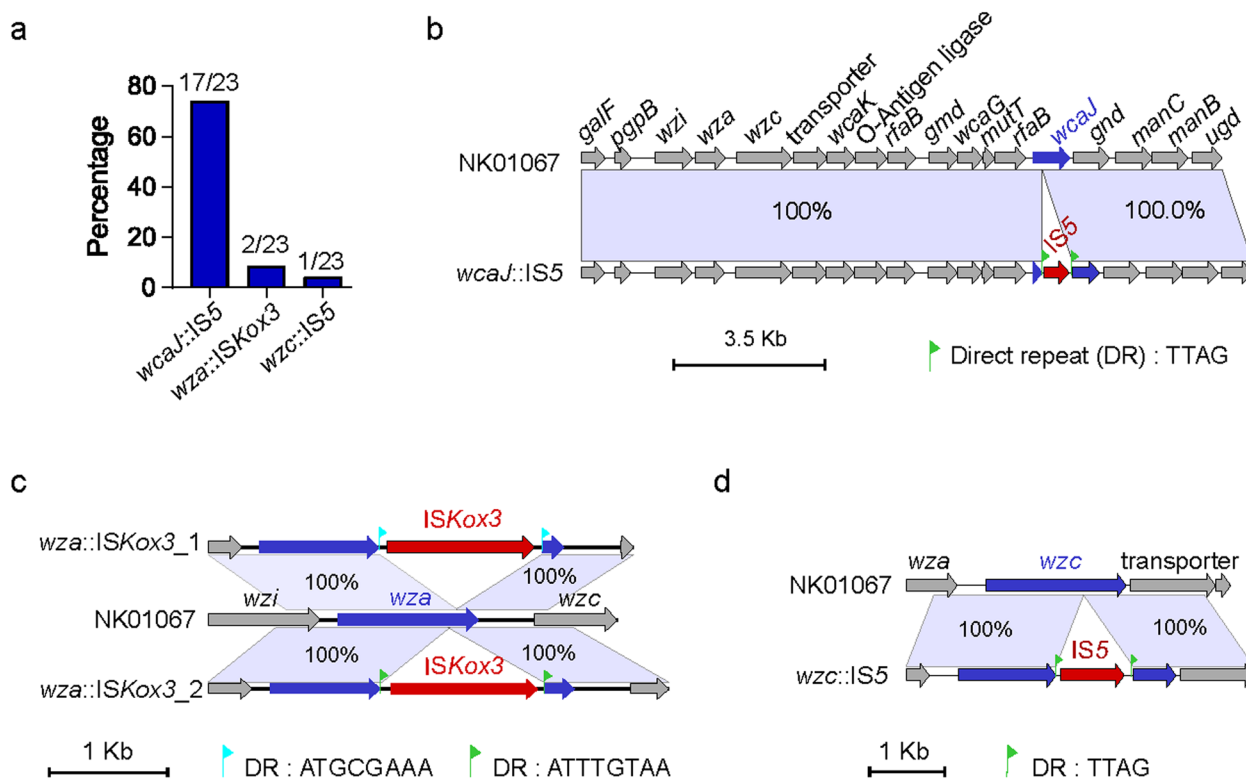


**Fig. 2** IS-mediated high-frequency inactivation of the CPS locus in NK01067 strain. **a** Proportion of NM-T colonies resulting from the inactivation of three genes—*wcaJ*, *wza*, and *wzc*—mediated by IS5 and ISKox3 elements. Sequence alignment of the K-loci between the wild type and mutants: **b** *wcaJ*::IS5, **c** *wza*::ISKox3, **d** *wzc*::IS5. IS elements are depicted in red. Direct repeats flanking IS elements are shown: 4 bp for IS5 and 8 bp for ISKox3

20 M–O colonies using PCR and did not observe any IS insertions in the CPS locus. To further verify these insertion patterns, we randomly selected three mutants with *wcaJ*::IS5, *wza*::ISKox3, and *wzc*::IS5 for whole-genome sequencing analysis (Additional file 1: Table S4). Consistent with the PCR results, only IS5 or ISKox3 were identified in the corresponding genes of the CPS locus, flanked by direct repeats (DRs) (TTAG for IS5, ATTTGTTAA or ATGCGAAAG for ISKox3) (Fig. 2b–d). No other IS or mutations were found in the CPS locus of the three sequenced strains, and no IS insertions were detected outside of the CPS locus when compared to the wild-type strain. Furthermore, we conducted a genomic analysis of the other strains that did not exhibit differing colony phenotypes (Additional file 1: Table S2). Notably, these strains lack IS5 and ISKox3, which highlights the potential role of these elements in capsular phase variation.

To confirm that the insertion of IS5 into *wcaJ* leads to NM-T colony formation, we restored the wild-type *wcaJ* gene in the *wcaJ*::IS5 mutant and observed the reappearance of M–O colonies in the complemented strain. Additionally, we investigated the cause of CPS loss in the low-frequency CPS loss strain NK10012. PCR and sequencing results identified frameshift mutations in the

*wcaJ* gene in 14 of the 23 NM-T colonies, and the insertion of IS102 in *wcaJ* was found in one colony (Additional file 1: Table S5). These results indicate that IS5 and ISKox3-mediated inactivation of CPS synthesis genes leads to a high frequency of CPS loss.

### IS elements in the carbapenem resistance plasmid driving genomic evolution

To elucidate the source of the IS5 and ISKox3 elements responsible for capsule inactivation in NK01067, we conducted a tracing analysis. We discovered that the IncX3-type plasmid, designated pNK01067-NDM-1, which carries the *bla*<sub>NDM-1</sub> gene, also harbors both IS5 and ISKox3 (Additional file 2: Fig. S1). Additionally, IS5 was identified downstream of the proteasome-type protease gene on the chromosome. We analyzed 1791 complete genomes of *K. pneumoniae* and found that IS5 was not detected downstream of the proteasome-type protease gene in any of these genomes, suggesting that the chromosomal IS5 in strain NK01067 likely originates from the plasmid. Among these genomes, 196 strains (11%) harbored IS5 (Additional file 1: Table S6). Of these, 71 strains had IS5 located on the chromosome, while 167 strains carried it on plasmids, with 42 strains containing IS5

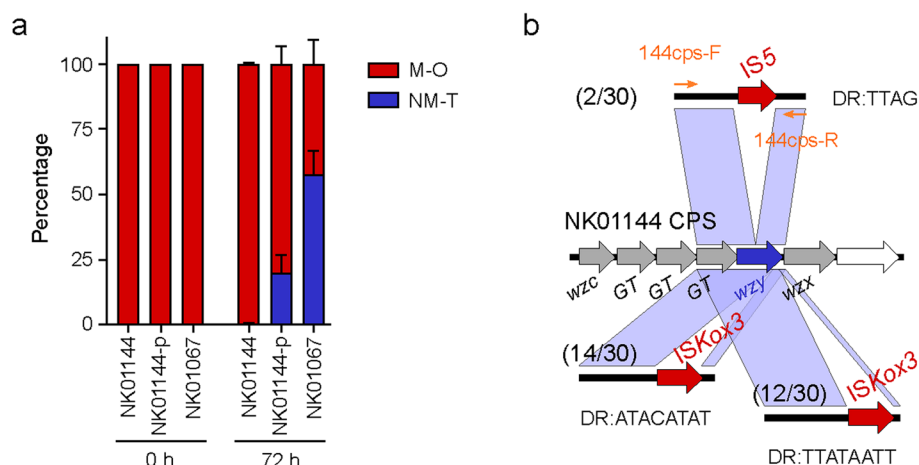


**Fig. 3** The acquisition of plasmid pNK01067-NDM- 1 in NK01144 results in an increased frequency of IS-mediated inactivation of the CPS locus. **a** The percentage of M–O and NM–T colonies present. **b** Sequence alignment of the K-loci between the wild type and mutants: among the 30 detected colonies, two were *wzy::IS5* and 26 were *wzy::ISKox3*. IS elements are depicted in red. Direct repeats (DR) flanking IS elements are shown: 4 bp for IS5 and 8 bp for ISKox3

on both plasmids and chromosomes. Among the plasmid-associated strains, 95 (48.5%) had IS5 on *bla*<sub>NDM</sub>-carrying plasmids, and 75.8% (72/95) of these plasmids co-harbored ISKox3. The majority of the *bla*<sub>NDM</sub>-carrying plasmids were of the IncX3 type, accounting for 65.3% (62/95). Additionally, we identified IS5 insertions within the capsule loci in 6 strains (3.1%) (Additional file 1: Table S6).

Furthermore, we analyzed the distribution of IS5 and ISKox3 across 285,417 bacterial genomes from 471 pathogenic species available in public databases (Global Catalogue of Microorganisms). IS5 was identified in 8204 genomes from 49 pathogenic species, with *E. coli* accounting for the majority at 60.2% (4938/8204) and *K. pneumoniae* as the second most prevalent at 13.4% (1100/8204). The earliest identification of IS5 in *E. coli* dates back to 1922 (with strains isolated from 1884 to 2022), and in *K. pneumoniae* to 2000 (with strains isolated from 1900 to 2022) (Additional file 2: Fig. S2a and Additional file 1: Table S7). ISKox3 was identified in 3867 genomes from 29 species, with *E. coli* accounting for 46.5% (1796/3867) and *K. pneumoniae* for 14.3% (553/3867). The earliest identification of ISKox3 in *Enterobacter hormaechei* dates back to 1929 (strains isolated from 1929 to 2023), and in *K. pneumoniae* to 2001 (Additional file 2: Fig. S2b and Additional file 1: Table S8). These data suggest that the IS5 and ISKox3 elements found in *K. pneumoniae* over the last 20 years may have originated from *E. coli* and *Enterobacter hormaechei*, likely via plasmid transfer, and have subsequently disseminated rapidly within *K. pneumoniae* populations.

To further validate that IS elements mediated by the *bla*<sub>NDM</sub>-carrying plasmid can promote capsular phase

variation, we selected the *K. pneumoniae* strain NK01144 (ST86, KL2, O1) for further study, which did not contain IS5 and ISKox3 and demonstrated low frequency (0.2%) of capsule loss in vitro passages for 72 h (Fig. 3a and Additional file 1: Table S2). The plasmid pNK01067-NDM- 1 was introduced into the NK01144 strain via electroporation, and transformants were selected using 4 mg/L meropenem. This procedure resulted in the NK01144 (pNK01067-NDM- 1) strain. After 72 h of serial passaging in vitro, the NM–T phenotype in the NK01144 (pNK01067-NDM- 1) strain occupied 20.0% of total colonies (Fig. 3a). Thirty randomly selected NM–T colonies were subjected to PCR and sequencing analysis, revealing that 93.3% (28/30) of these colonies contained IS insertions in the *wzy* gene (encoding polysaccharide polymerase) [33] (Fig. 3b). Specifically, 26 colonies exhibited ISKox3 insertions flanked by DR sequences ATACAT or TTATAATT, while 2 colonies exhibited IS5 insertions flanked by DR sequence TTAG (Fig. 3b). The *bla*<sub>NDM</sub>-carrying resistance plasmid not only significantly contributes to the dissemination of antibiotic resistance but also introduces novel elements such as IS5 and ISKox3. These insertion sequences play a critical role in the inactivation of capsular polysaccharide synthesis genes in *K. pneumoniae* strains like NK01067, thereby driving genomic dynamics and potentially facilitating bacterial adaptive evolution.

#### IS-mediated capsular phase variation leads to a significant increase in gene transfer frequency in vitro

We hypothesize that IS-mediated capsule loss may facilitate plasmid transfer between strains and accelerate the genomic convergence of multidrug resistance and

hypervirulence in *K. pneumoniae*. To test this hypothesis, we used wild-type (NK01067 *cap*<sup>+</sup>) and *wcaJ*::IS5 mutant (NK01067 *cap*<sup>-</sup>) strains as recipients, with *E. coli* UC1937 and *E. coli* S17 -1 as plasmid donors. UC1937 harbors the conjugative plasmid R388, carrying a trimethoprim resistance gene, and S17 -1 harbors the conjugative plasmid pK18 *mobsacB*, carrying a kanamycin resistance gene.

In conjugation experiments, the plasmid R388 was transferred into the *wcaJ*::IS5 mutant (NK01067 *cap*<sup>-</sup>) from *E. coli* UC1937 at an average frequency of  $(2.04 \pm 0.37) \times 10^{-1}$ , which is about 7.67  $\log_2$ -fold higher than the transfer frequency from UC1937 to NK01067 *cap*<sup>+</sup> (Fig. 4a). Meanwhile, the conjugation frequency of pK18 *mobsacB* from *E. coli* S17 -1 to NK01067 *cap*<sup>-</sup> was 2.49  $\log_2$ -fold higher than to NK01067 *cap*<sup>+</sup> (Fig. 4a). To assess the ability of *K. pneumoniae* to donate plasmids, we used wild-type and *wcaJ*::IS5 mutant strains carrying the conjugative plasmid pNK01067-NDM-1 as donors, with *E. coli* C600 (EC600) as the recipient. The average conjugal transfer frequency of pNK01067-NDM-1 from the *wcaJ*::IS5 mutant to EC600 was  $(1.48 \pm 0.39) \times 10^{-1}$ , which is 7.61  $\log_2$ -fold higher than from the wild-type strain to EC600 (Fig. 4b). This indicates that IS-mediated capsule locus deficiencies significantly increase conjugation efficiency. To further confirm the spread of pNK01067-NDM-1 between hvKP strains, we used another hvKP strain, RJF293H *cap*<sup>+</sup>, and its capsule-inactivated mutant RJF293H *cap*<sup>-</sup> (obtained via serial passaging in LB medium), as recipients. RJF293H (ST374, KL2, O1) does not carry resistance plasmids but harbors a non-conjugative pLVPK-like plasmid (pRJF293H) carrying canonical virulence determinants, including *rmrA*, *iro*, and *iuc* [10]. Using NK01067 *cap*<sup>+</sup> and *wcaJ*::IS5 mutant (NK01067 *cap*<sup>-</sup>) strains as donors, we found that the conjugal transfer of pNK01067-NDM-1 occurred only when both the donor (NK01067 *cap*<sup>-</sup>) and the recipient (RJF293H *cap*<sup>-</sup>) lacked capsules, albeit with a low average conjugation frequency of  $(4.17 \pm 3.62) \times 10^{-8}$ . Conjugation failed if either strain retained its capsule (Fig. 4b). These results are consistent with a recent study, which suggests that capsule type and volume account for most of the variation in the conjugation efficiency of *K. pneumoniae* [34].

To investigate whether pNK01067-NDM-1 could facilitate the transfer of the virulence plasmid pRJF293H, we used the Km-marked virulence plasmid host strain RJF293HK *cap*<sup>-</sup> with or without pNK01067-NDM-1 as donors, with EC600 as the recipient strain. The virulence plasmid was detected in the conjugates when RJF293HK *cap*<sup>-</sup> carrying pNK01067-NDM-1 was used as the donor, albeit at a low average frequency of  $(2.32 \pm 1.17) \times 10^{-7}$  (Fig. 4c). Transfer of the virulence plasmid was always

accompanied by co-conjugation of pNK01067-NDM-1. Conversely, no transfer of the virulence plasmid was observed when RJF293HK *cap*<sup>-</sup> without pNK01067-NDM-1 was used as the donor (Fig. 4c).

In addition to increased conjugation frequency, the IS-mediated capsule inactivation mutant exhibited enhanced fitness, with better growth and increased biofilm production in vitro compared to the wild-type parent (Additional file 2: Fig. S3a–b). This aligns with previous reports of non-encapsulated clones having significant fitness advantages in well-mixed, nutrient-rich environments [11, 35]. IS derived from the pNK01067-NDM-1 plasmid appears to promote capsule loss, thus enhancing fitness and competitiveness in vitro.

### Restoration of hypervirulence through loss of IS in capsule loci in vivo

Our previous study demonstrated that *K. pneumoniae* can persistently colonize the human intestine [36], while other studies suggest that capsule loss impairs gut colonization [37, 38]. IS elements encode transposases that excise them from the genome by cleaving DNA at their junctions. This raises the question of what happens when capsule-deficient mutants, resulting from IS insertion, colonize the gut. Specifically, could the IS5 element excise itself from the capsule gene and restore capsule production, thereby enhancing colonization?

To explore this, we constructed a long-term intestinal colonization model using nine 6–8-week-old SPF BALB/c mice, inoculated intragastrically with a dose of  $1 \times 10^8$  c.f.u. of the NK01067 *wcaJ*::IS5 mutant strain. The body weight of these mice showed an increasing trend consistent with the uninfected group (Fig. 5a). Fecal samples were collected at various time points (2, 6, 13, and 28 days post-infection) to detect intestinal colonization loads of *K. pneumoniae*. NM-T colonies were found in all samples on 2, 6, and 13 days post-infection (dpi). At 28 dpi, the colony phenotype changed, and M–O colonies were detected in samples from three mice (Fig. 5b). DNA sequencing of M–O colonies from these three mice demonstrated the excision of the IS5 element from the *wcaJ* gene, resulting in the complete reversion to the wild-type coding sequence in a scarless manner. Using the *wcaJ*::IS5 genome as a reference, SNP analysis identified three revertants with a limited number of SNPs (11, 19, and 11 SNPs). These SNPs were localized to two regions: (1) 11 SNPs located within 25 bp downstream of the *tRNA-Tyr* gene and (2) 8 SNPs in the terminal region of the *lamB* gene (Additional file 1: Table S9). This suggests that these colonies are indeed derived from the *wcaJ*::IS5 strain. Furthermore, among the nine mice colonized with the *wcaJ*::IS5 mutant, the intestinal colonization loads of *K. pneumoniae* in the three mice that isolated revertants

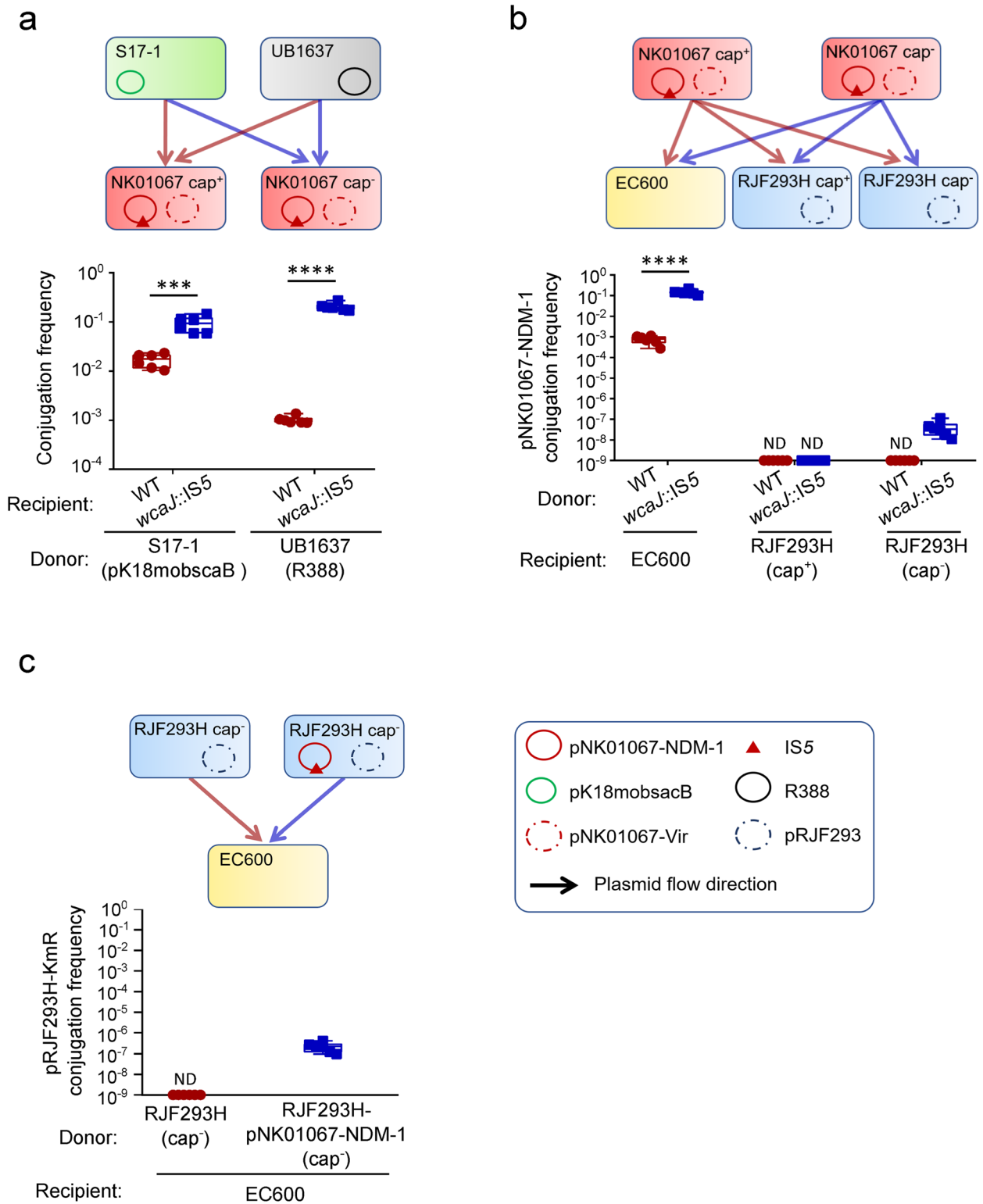


**Fig. 4** Conjugation frequency of plasmids. **a** Conjugation frequencies of plasmids pK18 mobsacB and R388 using NK01067 wild type (WT) and NK01067 *wcaJ::IS5* mutant as recipients, with S17-1 and UB1637 as donors. **b** Conjugation frequencies of plasmid pNK01067-NDM-1 with WT and *wcaJ::IS5* mutant as donors, and EC600, RJJF293H cap<sup>+</sup> (WT), and RJJF293H cap<sup>-</sup> (transparent strain after passage in LB medium) as recipients. **c** Conjugation frequencies of the virulence plasmid pRJJF293H with kanamycin resistance gene: RJJF293HK cap<sup>-</sup> (pRJJF293H-KmR) and RJJF293H cap<sup>-</sup> (pRJJF293H-KmR, pNK01067-NDM-1) as donors, with EC600 as the recipient. Each experiment was performed with at least five independent biological replicates. \*\*\*,  $p < 0.001$ ; \*\*\*\*,  $p < 0.0001$ ; ND, not detected

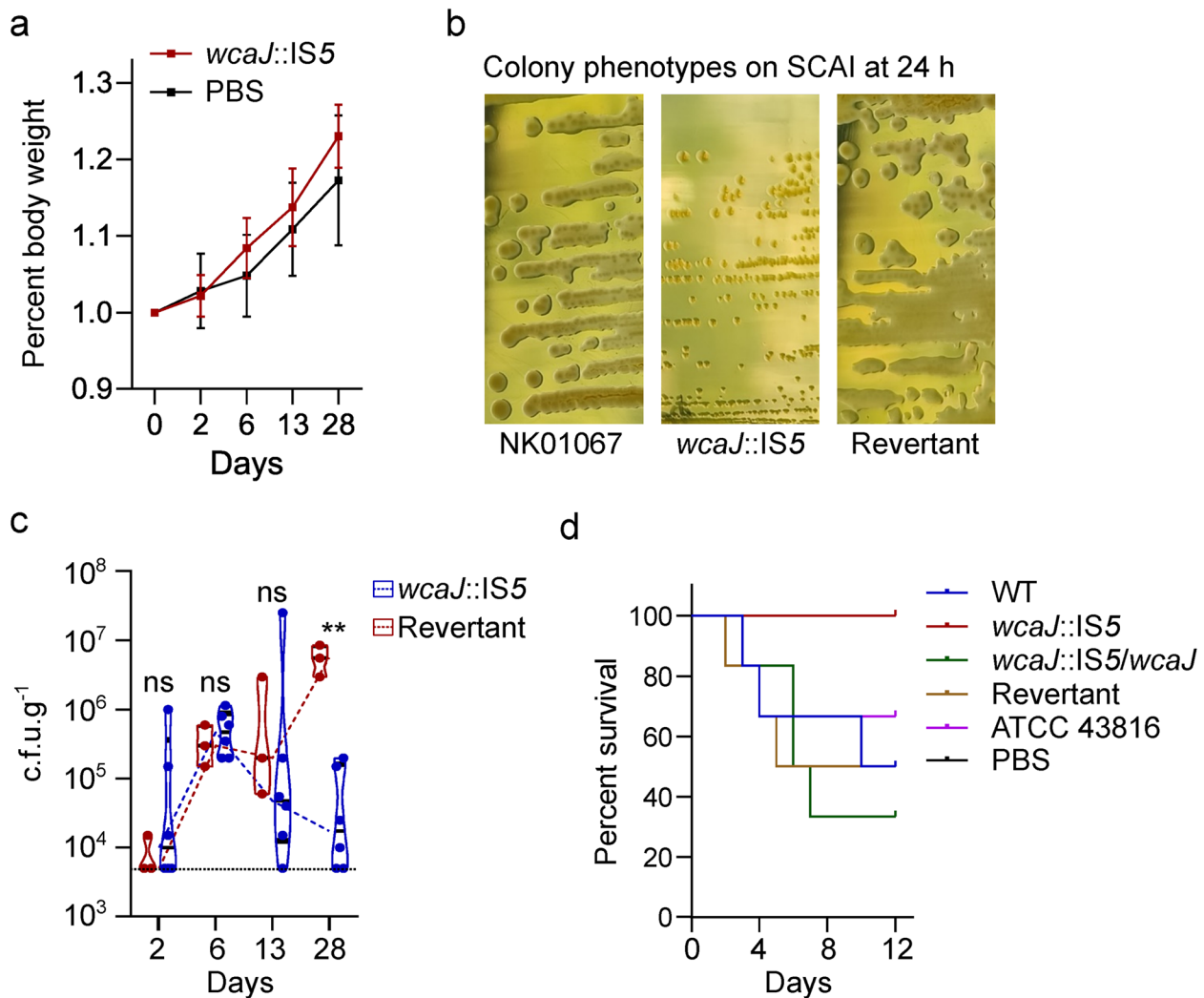


**Fig. 5** Restoration of hypervirulence through loss of IS in capsule loci in vivo. **a** Body weight change in mice infected with the *wcaJ::IS5* mutant ( $n = 9$  mice, individual measurements taken at different time points). **b** Colony phenotypes of NK01067 wild type, *wcaJ::IS5* mutant, and in vivo capsule-reverted strain (revertant) on Simmons citrate agar with 1% inositol (SCAI). **c** Fecal loads in 9 mice infected with the *wcaJ::IS5* mutant. Colonization levels in 3 mice with detectable revertant colonies (red) were compared to those in 6 mice without detectable revertant colonies (blue). For each mouse, 2–3 pellets were collected each time, and each sample underwent a single effective dilution and colony count. For samples below the detection limit, triplicate counts were conducted to ensure accuracy. The dashed line represents the detection limit ( $5 \times 10^3$  c.f.u./g). **d** Survival curve for mice infected with NK01067 wild type, *wcaJ::IS5* mutant, *wcaJ::IS5* in situ complemented strain (*wcaJ::IS5/wcaJ*), revertant, and ATCC43816. Each experimental group consisted of 6 mice. Error bars represent the standard error of the mean. \*\*,  $p < 0.01$ ; ns, not significant

ranged from  $3.0 \times 10^6$  to  $8.5 \times 10^6$  c.f.u.. In contrast, among the six mice that did not isolate revertants, two had NK01067 *wcaJ::IS5* loads below the detection limit, while the remaining four exhibited loads ranging from  $1.0 \times 10^4$  to  $2.0 \times 10^5$  c.f.u. (Fig. 5c). This suggests that the loss of IS and subsequent restoration of the capsule benefits gut colonization. A long-term experiment with wild-type NK01067 in the mouse gut also demonstrated that no capsule loss strains were detected over 20 days, further supporting the role of the capsule in intestinal colonization (Additional file 2: Fig. S4a–c).

Consistent with this, the *wcaJ::IS5* revertant restored to wild-type levels of mucoid phenotype, capsule production, growth, and biofilm production (Additional file 2: Fig. S3a–d). To examine the virulence of the revertant, an intragastric infection model was established, challenging mice with a dose of  $5 \times 10^7$  c.f.u. wide-type strain, the complementation strain (*wcaJ::IS5/wcaJ*), the *wcaJ::IS5* revertant, and *wcaJ::IS5* mutant strains were inoculated into mice separately. Additionally, *K. pneumoniae* ATCC 43816, which has been used extensively to model the *K. pneumoniae*-associated disease state in

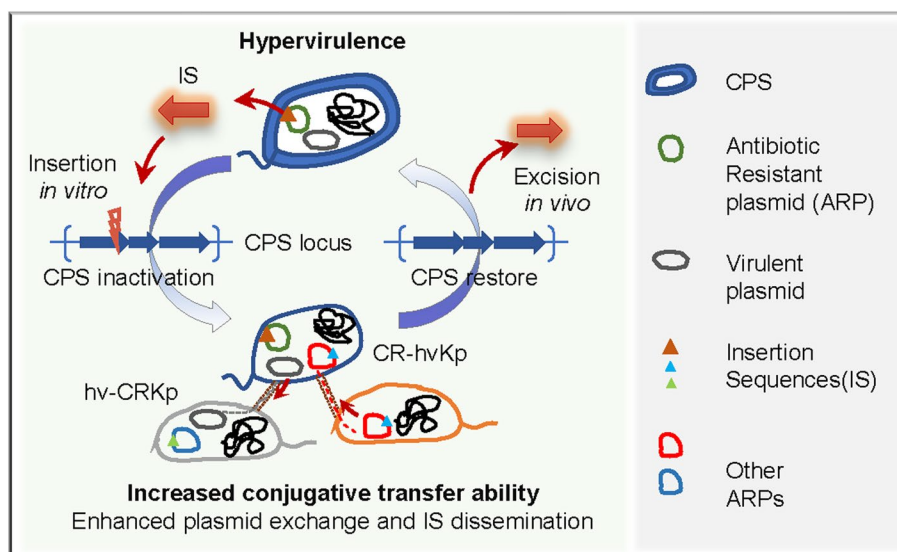


**Fig. 6** Overview of ISs accelerate genomic convergence of multidrug resistance and hypervirulence in *K. pneumoniae*. IS elements carried by carbapenem-resistant plasmids accelerate capsule inactivation, thereby enhancing plasmid exchange capabilities and promoting the prevalence of hypervirulence and multidrug-resistant *K. pneumoniae*. Through reciprocal plasmid exchange, IS elements rapidly spread and accumulate within the strain. Additionally, IS elements can self-excise *in vivo*, restoring CPS synthesis, and enhancing adaptability and virulence within the host

mice, was included as a control [37, 39]. The wild-type strain, complementation strain, and *wcaJ::IS5* revertant each caused  $\geq 50\%$  mortality within 12 dpi, while ATCC 43816 resulted in approximately 33% mortality within the same period (Fig. 5d). In contrast, the *wcaJ::IS5* mutant exhibited significantly reduced virulence, with no mortality observed within 12 dpi. These results indicate that the excision of IS5 from the capsule loci can restore capsule production *in vivo*, thereby enhancing the gut colonization and virulence of *K. pneumoniae*. IS elements confer remarkable flexibility in the dynamic relationship between capsule loss and restoration, which may significantly enhance the adaptability of *K. pneumoniae* across diverse host environments.

## Discussion

IS elements have long been considered selfish mobile genetic elements that primarily encode transposase for their own proliferation [40, 41]. Recent studies, however, have uncovered novel roles for IS elements as mechanisms to cope with external stress, which can trigger their transposition, leading to adaptive mutations and shaping bacterial evolution [42]. In this study, we demonstrated that IS elements mediate the ecological adaptive evolution (Fig. 6). Specifically, we show that IS5 and ISKox3 elements, likely originating from *Escherichia coli* and *Enterobacter hormaechei*, are transferred into *K. pneumoniae* via *bla*<sub>NDM-1</sub> plasmids and frequently insert into the CPS loci under LB culture conditions. In these nutrient-rich conditions, the loss of capsule production

confers a significant fitness advantage by reducing the metabolic burden associated with capsule biosynthesis, consistent with previous studies [11, 26]. Importantly, the reversible nature of IS insertion and excision enables a “bet-hedging” strategy, wherein *K. pneumoniae* can alternate between two phenotypic states: (1) capsule-on states for immune evasion in host environments and (2) capsule-off states that optimize conjugation efficiency, horizontal gene transfer, and biofilm formation. This capacity for dynamic adaptation allows *K. pneumoniae* to balance competing demands for virulence maintenance, resistance acquisition, and environmental fitness across diverse ecological niches. The capsule, while essential for overcoming host immunity and microbial competition *in vivo* [37, 38], may be suppressed in specific niches such as the urinary tract, where biofilm formation becomes a priority for persistent colonization [2]. However, further research is needed to investigate the precise spatiotemporal regulation of capsule phase variation during infection, which could reveal additional layers of complexity in the pathogen’s adaptation.

Since the first report of hypervirulent carbapenem-resistant *K. pneumoniae* (hv-CRKp) in 2018, there has been a growing body of literature documenting the convergence of virulence and resistance in *K. pneumoniae*, including hypervirulent strains acquiring resistance plasmids and drug-resistant clones obtaining virulence plasmids [2, 9, 43]. Our study provides critical mechanistic insights into the genomic convergence of multidrug resistance and hypervirulence in these pathogens. We

demonstrate that IS element-mediated capsule inactivation significantly enhances interbacterial plasmid transfer by removing the physical barrier to conjugation [34], thereby facilitating the horizontal dissemination of resistance and virulence determinants. While previous studies established that IncF plasmids can mediate virulence plasmid co-transfer through a piggyback mechanism, our work reveals that IncX3-type plasmids similarly promote this process [10]. These findings point to IS-mediated capsular phase variation as a potential mechanism promoting the genomic convergence of multidrug resistance and hypervirulence in *K. pneumoniae*.

## Conclusions

Our study demonstrates that plasmid-derived IS mediate dynamic capsule phase variation in CR-hvKP, acting as a genetic switch between (i) an encapsulated, virulent state that facilitates immune evasion and (ii) a non-encapsulated state that enhances horizontal plasmid transfer and biofilm formation. This bistable regulatory mechanism provides a plausible explanation for the rapid genomic convergence of virulence and resistance traits in CR-hvKP, an emerging and urgent public health threat.

## Supplementary Information

The online version contains supplementary material available at <https://doi.org/10.1186/s13073-025-01474-0>.

Additional file 1: Supplementary Tables S1–S9 (.xls). Table S1 Bacterial strains and plasmids used in this study. Table S2 Information of various hypervirulent *Klebsiella pneumoniae* strains. Table S3 Primer name and sequences used for PCR amplification in this study. Table S4 Sequencing analysis of *wcaJ*, *wza*, and *wzc* inserted by IS elements in NM-T colonies. Table S5 Mutations in the *wcaJ*, *wza*, and *wzc* genes detected in NM-T variants of NK10012 strain. Table S6 Locations of IS5 and its association with *bla<sub>NDM</sub>* in 196 *Klebsiella pneumoniae* strains. Table S7 Distribution of IS5 in 285,417 bacterial genomes of 471 pathogenic species from gcPathogen databases. Table S8 Distribution of ISKox3 in 285,417 bacterial genomes of 471 pathogenic species from gcPathogen databases. Table S9 SNP analysis of three revertants relative to the inoculated strain NK01067 *wcaJ*:IS5.

Additional file 2: Supplementary Figures S1–S4 (.pdf). Fig. S1 Circular representation of the IncX3-type resistance plasmid pNK01067-NDM-1. Fig. S2 Distribution and origin of IS5 and ISKox3 in pathogenic bacteria. Fig. S3 Phenotypic analysis of NK01067 wild type and its mutants. Fig. S4 Long-term colonization of mice with the wild-type strain NK01067.

## Acknowledgements

Not applicable.

## Authors' contributions

J.F. and D.-W.W. conceived the study. J.F. and D.-W.W. designed the experiments. D.-W.W., J.H., X.T. and C.W. performed molecular biology and bacteria experiments. D.-W.W., Y.S., Q.C. and L.W. performed bioinformatic analysis. J.F. and D.-W.W. wrote the manuscript with inputs from other contributing authors. J.F., Y.L. and G.Z. edited and finalized the manuscript. J.F. supervised the project. All authors have read and approved the manuscript.

## Funding

This study was supported by the National Key Research and Development Program of China (grant number 2022YFC2303100) and the International

Partnership Program of Chinese Academy of Sciences (grant number 079GJHZ2022033GC).

## Data availability

The whole-genome sequences of the six bacterial strains newly sequenced in this study are available for direct download from the National Center for Biotechnology Information (NCBI) under BioProject accession number PRJNA1135710. Complete genomes of *Klebsiella pneumoniae* strains carrying IS5, used for comparative analysis, were obtained from the NCBI RefSeq database, with accession numbers listed in Additional file 1: Table S6. Genomic data for pathogens carrying either IS5 or ISKox3 were retrieved from the gcPathogen database, a curated resource within the NMDC platform (<https://nmdc.cn/gcpathogen/pathogens?otherType=taxa&type=bacteria>) [24].

## Declarations

### Ethics approval and consent to participate

All animal experiments in this study were approved by the Ethics Committee of the Institute of Microbiology, Chinese Academy of Sciences (Approval No. APIMCAS2023077), and conducted in accordance with institutional and national guidelines for the care and use of laboratory animals. The research conformed to the principles of the Helsinki Declaration.

### Consent for publication

Not applicable.

### Competing interests

The authors declare no competing interests.

### Author details

<sup>1</sup>State Key Laboratory of Microbial Diversity and Innovative Utilization, Institute of Microbiology, Chinese Academy of Sciences, Beijing, China. <sup>2</sup>College of Life Science, University of Chinese Academy of Sciences, Beijing, China. <sup>3</sup>School of Clinical and Basic Medical Sciences, Shandong First Medical University & Shandong Academy of Medical Sciences, Jinan, Shandong, China.

Received: 22 July 2024 Accepted: 15 April 2025

Published online: 06 May 2025

## References

- Russo TA, Marr CM. Hypervirulent *Klebsiella pneumoniae*. *Clin Microbiol Rev.* 2019;32:32.
- Ernst CM, Braxton JR, Rodriguez-Osorio CA, Zagieboylo AP, Li L, Pironti A, Manson AL, Nair AV, Benson M, Cummins K, et al. Adaptive evolution of virulence and persistence in carbapenem-resistant *Klebsiella pneumoniae*. *Nat Med.* 2020;26:705–11.
- Shrivastava S, Shrivastava P, Ramasamy J. World Health Organization releases global priority list of antibiotic-resistant bacteria to guide research, discovery, and development of new antibiotics. *J Med Soc.* 2017;32:32.
- Choby JE, Howard-Anderson J, Weiss DS. Hypervirulent *Klebsiella pneumoniae* - clinical and molecular perspectives. *J Intern Med.* 2020;287:283–300.
- Pu D, Zhao J, Chang K, Zhuo X, Cao B. "Superbugs" with hypervirulence and carbapenem resistance in *Klebsiella pneumoniae*: the rise of such emerging nosocomial pathogens in China. *Sci Bull (Beijing).* 2023;68:2658–70.
- Hu F, Pan Y, Li H, Han R, Liu X, Ma R, Wu Y, Lun H, Qin X, Li J, et al. Carbapenem-resistant *Klebsiella pneumoniae* capsular types, antibiotic resistance and virulence factors in China: a longitudinal, multi-centre study. *Nat Microbiol.* 2024;9:814–29.
- Li J, Ren J, Wang W, Wang G, Gu G, Wu X, Wang Y, Huang M, Li J. Risk factors and clinical outcomes of hypervirulent *Klebsiella pneumoniae* induced bloodstream infections. *Eur J Clin Microbiol Infect Dis.* 2018;37:679–89.
- Wyres KL, Lam MMC, Holt KE. Population genomics of *Klebsiella pneumoniae*. *Nat Rev Microbiol.* 2020;18:344–59.

9. Liu L, Lou N, Liang Q, Xiao W, Teng G, Ma J, Zhang H, Huang M, Feng Y. Chasing the landscape for intrahospital transmission and evolution of hypervirulent carbapenem-resistant *Klebsiella pneumoniae*. *Sci Bull (Beijing)*. 2023;68:3027–47.
10. Xu Y, Zhang J, Wang M, Liu M, Liu G, Qu H, Liu J, Deng Z, Sun J, Ou HY, Qu J. Mobilization of the nonconjugative virulence plasmid from hypervirulent *Klebsiella pneumoniae*. *Genome Med*. 2021;13:119.
11. Nucci A, Rocha EPC, Rendueles O. Adaptation to novel spatially-structured environments is driven by the capsule and alters virulence-associated traits. *Nat Commun*. 2022;13:4751.
12. Wang S, Ding Q, Zhang Y, Zhang A, Wang Q, Wang R, Wang X, Jin L, Ma S, Wang H. Evolution of virulence, fitness, and carbapenem resistance transmission in ST23 hypervirulent *Klebsiella pneumoniae* with the capsular polysaccharide synthesis gene *wcaI* inserted via insertion sequence elements. *Microbiol Spectr*. 2022;10: e0240022.
13. Siguier P, Gourbeyre E, Chandler M. Bacterial insertion sequences: their genomic impact and diversity. *FEMS Microbiol Rev*. 2014;38:865–91.
14. Si M, Zhao C, Burkinshaw B, Zhang B, Wei D, Wang Y, Dong TG, Shen X. Manganese scavenging and oxidative stress response mediated by type VI secretion system in *Burkholderia thailandensis*. *Proc Natl Acad Sci U S A*. 2017;114:E2233–e2242.
15. Wang Y, Wang S, Chen W, Song L, Zhang Y, Shen Z, Yu F, Li M, Ji Q. CRISPR-Cas9 and CRISPR-assisted cytidine deaminase enable precise and efficient genome editing in *Klebsiella pneumoniae*. *Appl Environ Microbiol*. 2018;84:e01834-18.
16. Pribelski A, Antipov D, Meleshko D, Lapidus A, Korobeynikov A. Using SPAdes de novo assembler. *Curr Protoc Bioinformatics*. 2020;70: e102.
17. Siguier P, Perochon J, Lestrade L, Mahillon J, Chandler M. ISfinder: the reference centre for bacterial insertion sequences. *Nucleic Acids Res*. 2006;34:D32–36.
18. Carattoli A, Zankari E, García-Fernández A, Voldby Larsen M, Lund O, Villa L, Møller Aarestrup F, Hasman H. In silico detection and typing of plasmids using PlasmidFinder and plasmid multilocus sequence typing. *Antimicrob Agents Chemother*. 2014;58:3895–903.
19. Grant JR, Enns E, Marinier E, Mandal A, Herman EK, Chen CY, Graham M, Van Domselaar G, Stothard P. Proksee: in-depth characterization and visualization of bacterial genomes. *Nucleic Acids Res*. 2023;51:W484–w492.
20. Sullivan MJ, Petty NK, Beatson SA. Easyfig: a genome comparison visualizer. *Bioinformatics*. 2011;27:1009–10.
21. Inkscape.org: Frequently asked questions-for Inkscape. Available online: <https://inkscape.org/>. Accessed 1 Apr 2020.
22. Altschul SF, Gish W, Miller W, Myers EW, Lipman DJ. Basic local alignment search tool. *J Mol Biol*. 1990;215(3):403–10. [https://doi.org/10.1016/S0022-2836\(05\)80360-2](https://doi.org/10.1016/S0022-2836(05)80360-2).
23. Jolley KA, Bray JE, Maiden MCJ. Open-access bacterial population genomics: BIGSdb software, the PubMLST.org website and their applications. *Wellcome Open Res*. 2018;3:124.
24. Guo C, Chen Q, Fan G, Sun Y, Nie J, Shen Z, Meng Z, Zhou Y, Li S, Wang S, Ma J, Sun Q, Wu L: gcPathogen: a comprehensive genomic resource of human pathogens for public health. *Nucleic Acids Res*. 2023. <https://nmdc.cn/gcpathogen/>.
25. Liu C, Dong N, Huang X, Huang Z, Cai C, Lu J, Zhou H, Zhang J, Zeng Y, Yang F, et al. Emergence of the clinical rdar morphotype carbapenem-resistant and hypervirulent *Klebsiella pneumoniae* with enhanced adaptation to hospital environment. *Sci Total Environ*. 2023;889: 164302.
26. Vezina B, Cooper HB, Wisniewski JA, Parker MH, Jenney AWJ, Holt KE, Wyres KL. Wild-type domestication: loss of intrinsic metabolic traits concealed by culture in rich media. *Microb Ecol*. 2024;87:144.
27. Guo X, Chen R, Wang Q, Li C, Ge H, Qiao J, Li Y. Global prevalence, characteristics, and future prospects of IncX3 plasmids: a review. *Front Microbiol*. 2022;13: 979558.
28. Campos JC, da Silva MJ, dos Santos PR, Barros EM, Pereira Mde O, Seco BM, Magagnin CM, Leiroz LK, de Oliveira TG, de Faria-Júnior C, et al. Characterization of Tn3000, a transposon responsible for *bla*<sub>NDM-1</sub> dissemination among Enterobacteriaceae in Brazil, Nepal, Morocco, and India. *Antimicrob Agents Chemother*. 2015;59:7387–95.
29. Acman M, Wang R, van Dorp L, Shaw LP, Wang Q, Luhmann N, Yin Y, Sun S, Chen H, Wang H, Balloux F. Role of mobile genetic elements in the global dissemination of the carbapenem resistance gene *bla*<sub>NDM-1</sub>. *Nat Commun*. 2022;13:1131.
30. Chin CY, Tipton KA, Farokhyfar M, Burd EM, Weiss DS, Rather PN. A high-frequency phenotypic switch links bacterial virulence and environmental survival in *Acinetobacter baumannii*. *Nat Microbiol*. 2018;3:563–9.
31. Chiarelli A, Cabanel N, Rosinski-Chupin I, Zongo PD, Naas T, Bonnin RA, Glaser P. Diversity of mucoicid to non-mucoicid switch among carbapenemase-producing *Klebsiella pneumoniae*. *BMC Microbiol*. 2020;20:325.
32. He J, Shi Q, Chen Z, Zhang W, Lan P, Xu Q, Hu H, Chen Q, Fan J, Jiang Y, et al. Opposite evolution of pathogenicity driven by *in vivo* *wzc* and *wcaI* mutations in ST11-KL64 carbapenem-resistant *Klebsiella pneumoniae*. *Drug Resist Updat*. 2023;66: 100891.
33. Ovchinnikova OG, Treat LP, Teelucksingh T, Clarke BR, Miner TA, Whitfield C, Walker KA, Miller VL. Hypermucoviscosity regulator RmpD interacts with Wzc and controls capsular polysaccharide chain length. *mBio*. 2023;14:e0080023.
34. Haudiquet M, Le Bris J, Nucci A, Bonnin RA, Domingo-Calap P, Rocha EPC, Rendueles O. Capsules and their traits shape phage susceptibility and plasmid conjugation efficiency. *Nat Commun*. 2024;15:2032.
35. Buffet A, Rocha EPC, Rendueles O. Nutrient conditions are primary drivers of bacterial capsule maintenance in *Klebsiella*. *Proc Biol Sci*. 2021;288:20202876.
36. Yang J, Li Y, Tang N, Li J, Zhou J, Lu S, Zhang G, Song Y, Wang C, Zhong J, et al. The human gut serves as a reservoir of hypervirulent *Klebsiella pneumoniae*. *Gut Microbes*. 2022;14: 2114739.
37. Young TM, Bray AS, Nagpal RK, Caudell DL, Yadav H, Zafar MA. Animal model to study *Klebsiella pneumoniae* gastrointestinal colonization and host-to-host transmission. *Infect Immun*. 2020;88:10.
38. Favre-Bonté S, Licht TR, Forestier C, Krogfelt KA. *Klebsiella pneumoniae* capsule expression is necessary for colonization of large intestines of streptomycin-treated mice. *Infect Immun*. 1999;67:6152–6.
39. Bachman MA, Breen P, Deornellas V, Mu Q, Zhao L, Wu W, Cavalcoli JD, Mobley HL. Genome-wide identification of *Klebsiella pneumoniae* fitness genes during lung infection. *mBio*. 2015;6:e00775.
40. Sheng Y, Wang H, Ou Y, Wu Y, Ding W, Tao M, Lin S, Deng Z, Bai L, Kang Q. Insertion sequence transposition inactivates CRISPR-Cas immunity. *Nat Commun*. 2023;14:4366.
41. Doolittle WF, Sapienza C. Selfish genes, the phenotype paradigm and genome evolution. *Nature*. 1980;284:601–3.
42. Wei DW, Wong NK, Song Y, Zhang G, Wang C, Li J, Feng J. IS26 veers genomic plasticity and genetic rearrangement toward carbapenem hyperresistance under sublethal antibiotics. *mBio*. 2021;13:e0334021.
43. Gu D, Dong N, Zheng Z, Lin D, Huang M, Wang L, Chan EW, Shu L, Yu J, Zhang R, Chen S. A fatal outbreak of ST11 carbapenem-resistant hypervirulent *Klebsiella pneumoniae* in a Chinese hospital: a molecular epidemiological study. *Lancet Infect Dis*. 2018;18:37–46.

## Publisher's Note

Springer Nature remains neutral with regard to jurisdictional claims in published maps and institutional affiliations.